Virchows Archiv A Pathol Anat (1992) 420:5–10

Virchows Archiv A
Pathological Anatomy and Histopathology

Ultrastructural observations on cytotoxic effector cells infiltrating pancreatic islets of low-dose streptozocin treated mice

Gianpaolo Papaccio and Vincenzo Esposito

Institute of Anatomy, I School of Medicine, via L. Armanni, 5, I-80138 Naples, Italy

Received March 4, 1991 / Received after revision July 30, 1991 / Accepted July 31, 1991

Summary. The aim of this study was to observe the ultrastructural events, during the onset of diabetes mellitus in the low-dose streptozocin (LDS)-treated mouse model with emphasis on the infiltrating elements. Forty male C57 BL/6J mice were given 40 mg/streptozocin on 5 consecutive days and killed 5, 6, 7, 8, 9, 10, 15, and 18 days after the first injection. Results demonstrated that islet infiltration occurring in LDS-treated mice is characterized by a very early pre-infiltration state in which mononuclear phagocytes in islet capillary vessels were considerably increased in number. A new histopathological time sequence for the early insulitis is described, in which attraction of blood mononuclear phagocytes into the islet capillary lumen is the first step. During the successive stage, occurring on days 6–8 we observed that mononuclear phagocytes migrate through capillary and venule walls into the islet parenchyma, where they differentiate into tissue macrophages. It was only later (step 3) that these macrophages acquired novel properties, typical of their "activated state" and started to phagocytose islet beta-cell debris. These data suggest that during the pre-infiltration and early insulitis the mononuclear phagocyte system plays a key role in the onset of LDS diabetes.

Key words: Islets of Langerhans – Monocytic phagocytes – Streptozocin – Type 1 diabetes – Ultrastructure

Introduction

Like and Rossini (1976) described a new model of insulin-dependent diabetes mellitus (IDDM) obtained in mice given multiple low doses of streptozocin (LDS). Diabetes induced in animals using this technique is a frequently used model of autoimmune diabetes (Like et al. 1978; Kolb 1987) and is accompanied by an islet infiltrate often called "insulitis", the inflammatory cells of which (mainly described by them as lymphocytes) selectively destroy the insulin-containing beta-cells. More than 10 years after the first description, Kolb-Bachofen and co-workers (1988) studied the early stages of the infiltration at the electron microscopic level and described a step by step mechanism in which macrophages played a role as the first element attacking the islet beta-cells. Further studies have confirmed these observations (Walker et al. 1988) and we have recently found that "recruited" macrophages play an important role in the early islet infiltration (Papaccio et al. 1991). It is also known that specific killer cells are able to lyse the appropriate targets by direct contact: among the killer cells cytotoxic T-lymphocytes (CTL), lymphokine-activated killer (LAK) and natural killer (NK) cells are also effective in the lysis of targets and may therefore be effective against the islet beta-cells (Groscurth 1989).

Histopathological time sequence data indicate that in the spontaneous diabetes occurring in BB rats and NOD mice, macrophages are the first inflammatory cell population to invade the islet, before B-lymphocytes, T-lymphocytes or NK cells and disease onset (Charlton et al. 1988; Lee et al. 1988a. b; Hanenberg et al. 1989).

The exact role of the immune elements infiltrating the islet is unclear, even though it is assumed that cytolysis and phagocytosis occur. Moreover, it has been demonstrated that in the early stage after LDS treatment islet vasoconstriction may occur (Papaccio et al. 1990) and this phenomenon may play a key role during onset. The aim of the present work was to elucidate the ultrastructural features of the infiltrating elements in LDS-treated mice in a day-by-day study. In particular, we also studied the very early state of infiltration during the "single cell insulitis" and the relationship between macrophages, islet microvasculature and other cytotoxic effector cells in the affected islets.

Materials and methods

A total of 40 male C57 BL/6J mice bred in our institute were used. The animals, aged between 10 and 15 weeks, were fed ad

Offprint requests to: G. Papaccio

libitum and were checked daily for serum glucose. Four animals were given saline and used as controls. The remaining animals were treated with intra-peritoneal injections of 40 mg streptozocin (STZ)/kg body weight (Zanosar, Upjohn Milan, Italy) on 5 consecutive days as previously described (Like and Rossini 1976; Papaccio et al. 1986; Papaccio and Mezzogiorno 1989). Animals were classed as diabetics when glycaemia exceeded 11 mmol glucose/l (Glucoquant, Boehringer, Mannheim, FRG). On days 5, 6, 7, 8, 9, 10, 15 and 18 after the first STZ injection animals ($n=4$ per day) were anaesthetized and the pancreas removed and cut into small cubes. Samples were immediately fixed in a 0.1 M phosphate buffered solution of 3.75% paraformaldehyde and 1.25% glutaraldehyde (pH 7.38) for 2 h at 4° C, then washed and post-fixed in 1% osmium tetroxide in the same buffered solution for 1 h at 4° C. Specimens were then dehydrated and embedded in epoxy resin ready for sectioning under a LKB ultratome. The first 4 islets encountered in the semi-thin sections of the pancreas of each treated ($n=36$) and control ($n=4$) animals were examined and screened for ultra-thin sectioning. A total of 160 islets were ultrastructurally observed. Counterstained ultra-thin sections were examined under a Zeiss EM 109 electron microscope (Zeis, Jena, FRG).

Results

Control animals showed normal glycaemic values (see Table 1) throughout the experiment. LDS-treated mice were found to be normoglycaemic on days 5–10. A rise in glycaemia was observed on day 15 but values still remained below 11 mmol/l. The animals became hyperglycaemic on day 18 with values ranging around 10 mmol/l ($P<0.001$ vs controls).

The ultrastructure of the islets of control mice was, as expected, normal: no cell necrosis or degranulation were seen. Islet beta-cells showed a normal morphology: they were polyhedral in shape with a round or slightly oval nucleus. Slender and rod-shaped mitochondria were numerous and many mature and immature secretory granules were seen scattered in the cytoplasm; the Golgi apparatus was usually large. No infiltrated islets were found. Semi-quantitative results (see Table 2) show that only 7 monocytes in 3 islets (2, 3 and 2 respectively) were observed. Two unactivated macrophages were also detected in 2 islets (1 per islet). No phagocytosing macrophages were seen.

In LDS-treated animals on day 5 the majority of islet capillary vessels in 12 of 16 of the islets exlamined showed many blood monocytes that, sometimes, seemed to occlude the lumen. These mononuclear macrophage precursors showed a relatively large, euchromatic nucleus with typical indentations on one side (Fig. 1). Approximately 90% of vessels of all the islets belonging to 3 of 4 animals presented these elements. Usually 1 or 2 monocytes per vessel per section were encountered so that in each section 5–10 monocytes were detected. The islets of the remaining animals showed fewer monocytes with a variable distribution within the islets, ranging from 0 to a maximum of 10 monocytes per section.

Infiltrating elements could also be seen within or, more frequently, around the islets: these cells had the appearance of non-activated macrophages (Fig. 2). They did not contain secondary lysosomes or vacuoles with cells debris. No lymphocytes or other cytotoxic effector cells were observed. Islet beta-cells still appeared normal; however, a partial degranulation or slight cytoplasmic vacuolation was seen in some cases.

By day 6–8 no substantial modifications had occurred with regard to the ultrastructure of islet beta-cells: these elements showed a discrete degranulation only in some

Table 1. Glycaemic blood levels in treated mice

Day	Glycaemia (mmol/l) mean ± SD	Day	Glycaemia (mmol/l) mean ± SD
0	5.51 ± 0.3	9	6.33 ± 0.2
5	5.53 ± 0.2	10	6.45 ± 0.3
6	5.57 ± 0.3	15	8.85 ± 0.9
7	5.62 ± 0.2	18	10.88 ± 0.5
8	5.96 ± 0.3		

Table 2. Semi-quantitative data on islet infiltration

Day examined	Infiltration		
	% of examined islets showing infiltration	% of animals sacrificed with infiltrated islets	Type of infiltrating cell
Controls	0	0	–
5	75	75	Intravascular monocytes
6–8	83	83	Activated intra-islet macrophages
9, 10	83	89	Phagocytozing macrophages and few lymphocytes
15–18	78	75	Lymphocytes and few macrophages

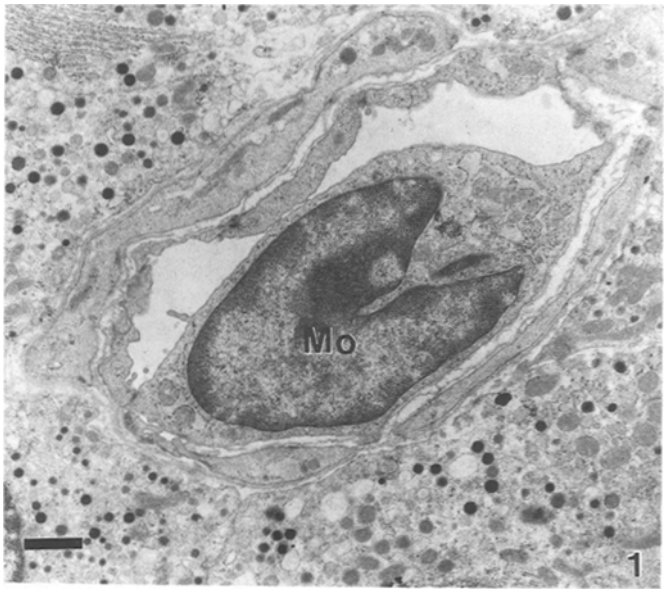

Fig. 1. Photomicrograph showing an intravascular monocyte (*Mo*), day 5. *Bar* = 0.9 μm; ×4400

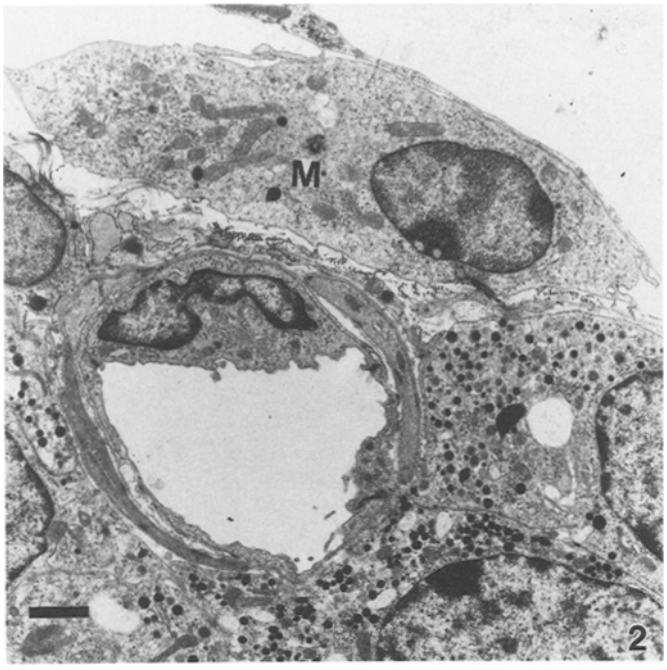

Fig. 2. Photomicrograph of a macrophage (*M*) in a peri-islet position, day 5. *Bar* = 0.8 μm; × 3000

cases but mitochondria and other organelles were normal. However, very important changes occurred in and around the islet capillary vessels. Capillary lumina and perivascular areas showed an increase of mononuclear phagocytes that were seen to undergo a morpho-functional differentiation into tissue macrophages. In fact, several mononuclear phagocytes were seen exiting the vessels and entering the islet parenchyma where they acquired protrusions and other features typical of the "activated state" of macrophages. They all appeared as large cells which contained rough and smooth endoplasmic reticulum, an active Golgi apparatus, mitochondria, endocytic vesicles and a large euchromatic nucleus (Fig. 3). Semi-quantitative data show that all of the islets examined in 10 of 12 animals showed an increased number of monocytes (10–15/section) and activated macrophages. The remaining 2 animals showed a smaller amount of these elements (from 0–2 to 5–8 per section).

By days 9 and 10 the most interesting changes had occurred. All the islets examined had activated macrophages, and many of these (at least 5 to a maximum of 8 macrophages per section) were seen to have begun phagocytosis of islet beta-cells: in fact macrophages containing phagocytosed islet beta-cell debris with still recognizable typical beta-granules within them were seen (Fig. 4). In some cases several granule cores had a crystal-like bar instead of the usual appearance (Fig. 5). Degenerating membranes were also seen within the phagosomes. Furthermore, single non-activated macrophages were seen scattered throughout the islets, mainly in a vascular position (Fig. 6). Among the other cytotoxic effector cells lymphocytes were only rarely encountered (Fig. 7).

Undamaged and damaged islet beta-cells, without the presence of macrophages or other cytotoxic effector cells, were seen next to each other within the same islet. The damaged beta-cells showed a dilated Golgi apparatus, swollen mitochondria and a variable degree of degranulation and vacuolation.

At day 15 and 18 the majority of the islet beta-cells were considerably damaged: swollen mitochondria, vacuolation and marked degranulation were observed. Islet

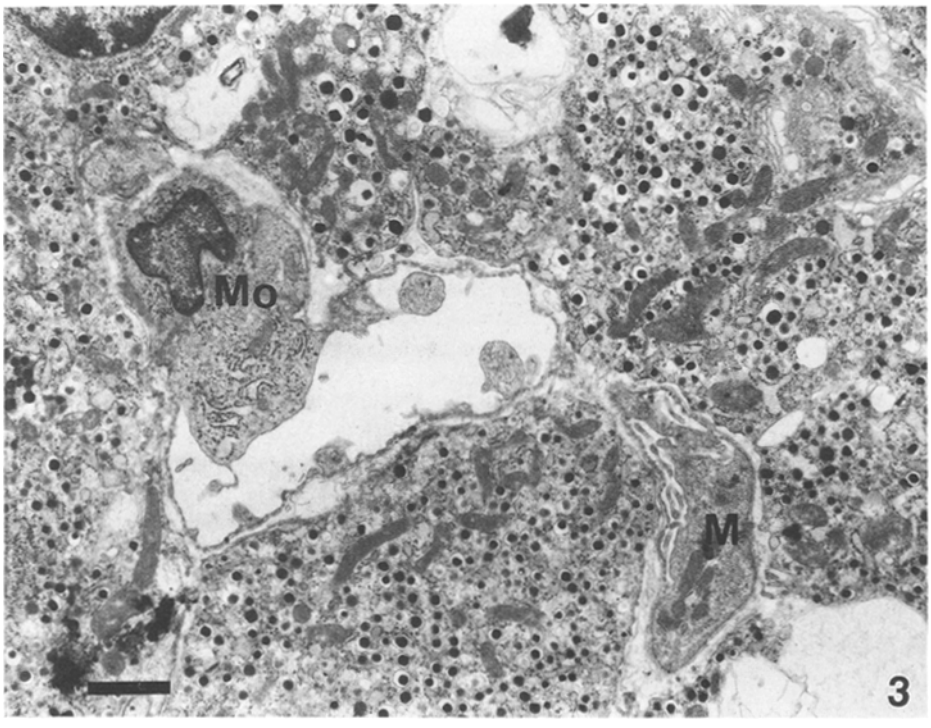

Fig. 3. Photomicrograph showing a phagocytic monocyte (*Mo*) exiting an intra-islet capillary. An activated macrophage (*M*) with typical protrusions that has just exited the capillary can also be seen, day 8. *Bar* = 0.8 μm; × 3000

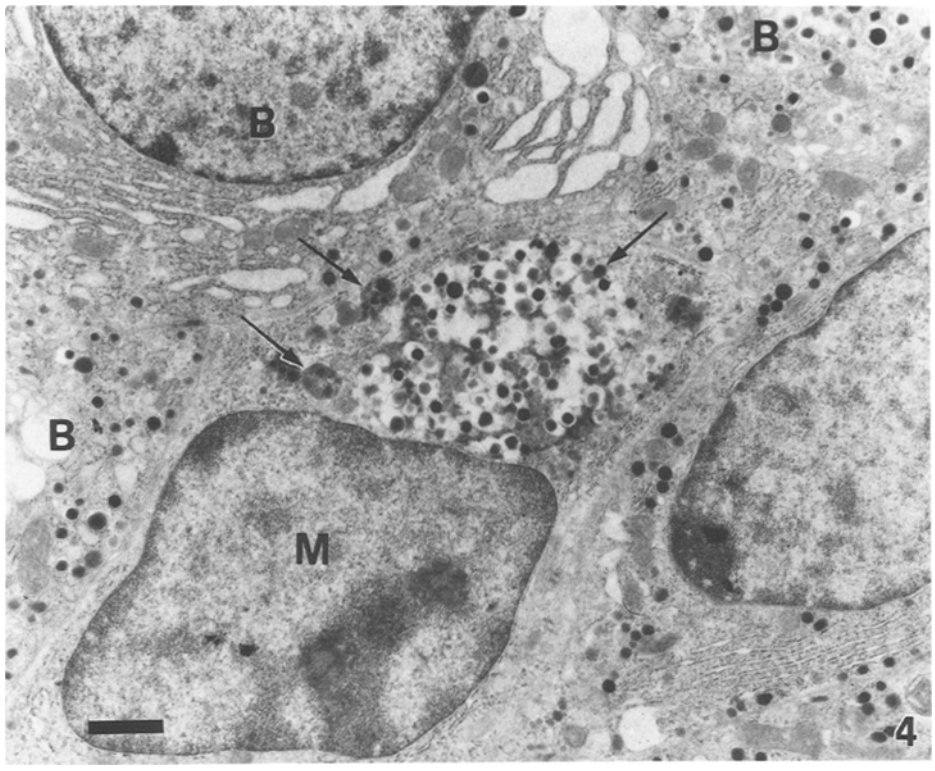

Fig. 4. Photomicrograph showing phagocytosed islet beta-cell debris (*arrows*) within a macrophage (*M*) next to a degranulated and vacuolated islet beta-cell at day 9. *Bar* = 0.6 μm; × 3000

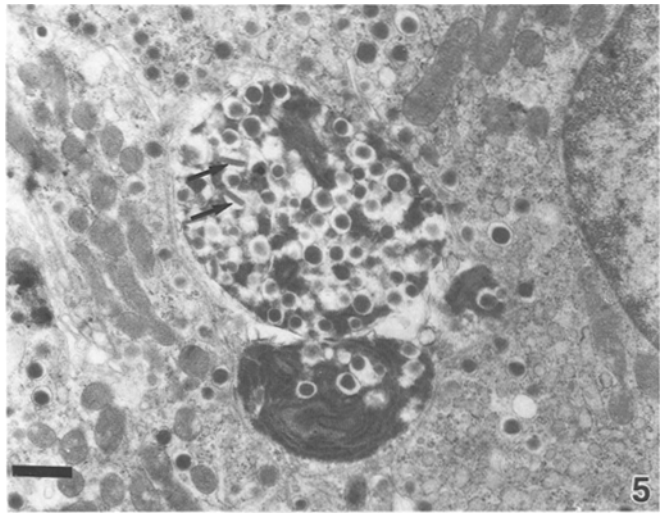

Fig. 5. Photomicrograph of phagocytosed beta-cell debris showing granules containing crystal-like bars (*arrows*). *Bar* = 1.4 μm; × 7000

beta-cell nuclei were often smaller than normal with an irregular profile (Fig. 8).

Macrophages were seen only rarely but other cytoxic effector cells were observed more frequently. These included mainly lymphocytes (Fig. 8) (seen in 6/8 animals; 25/32 islets examined; numbers ranged from 3–4 to 8 lymphocytes per section) and several subpopulations of them like CTL, NK cells and LAK cells. These elements showed lysosomes of different types and membrane vesicles with parallel tubular arrays. Actually LAK cells, NK cells and CTL showed a marked heterogeneity and were difficult to identify morphologically.

Discussion

This study has clearly demonstrated that islet infiltration in LDS-treated mice is characterized by a very early pre-infiltration state (already ongoing 5 days after the first STZ injection) in which mononuclear phagocytes in islet capillary vessels are considerably increased in number. Therefore, we can describe a new histopathological time sequence for the early insulitis in which attraction of blood mononuclear phagocytes into the islet capillary lumen is the first step. This follows unknown stimulation consistent with autoimmune processes.

During the successive stage, occuring on days 6–8, we observed that these elements, described as mononuclear phagocytes, migrate through capillary and venule walls into the islet parenchyma where they differentiate into tissue macrophages. Only later (step 3) do these macrophages acquire novel properties, typical of their activated state, and start to phagocytose islet beta-cell debris. In a previous study (Papaccio et al. 1991) we hypothesized that recruited macrophages instead of resident macrophages, as proposed by Kolb-Bachofen et al. (1988), have a greater importance in attacking islet beta-cells. The above-described histopathological time sequence of the pre-infiltration and early insulitis now gives the mononuclear phagocyte system a key role in the pathogenesis of LDS diabetes.

The mononuclear phagocyte system, consisting of monocytes and tissue macrophages, is the major cellular component of the classical reticuloendothelial system. It is a generally dynamic cellular system having the potential to exert a modulatory role in tissue homeostasis in local immunological and inflammatory responses. These phagocytes are highly active cells that readily re-

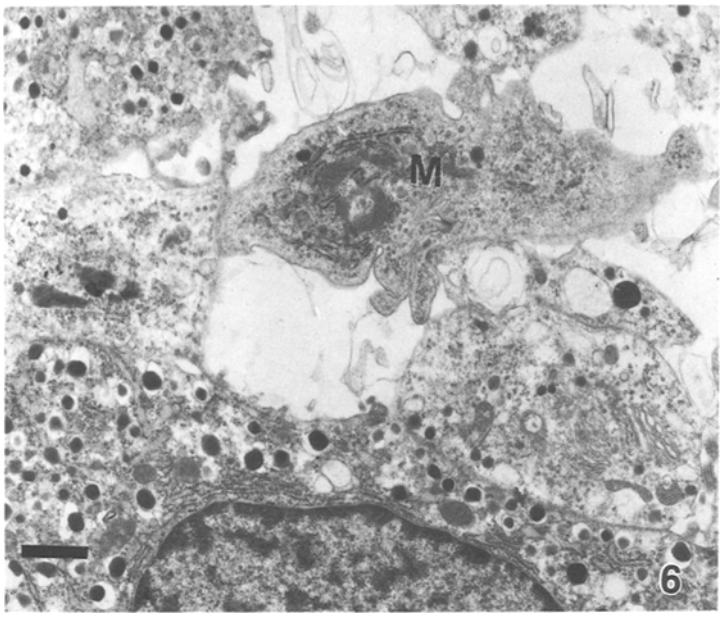

Fig. 6. Photomicrograph showing a macrophage (*M*), with ruffled membranes typical of an activated state, in a vascular position, day 10. *Bar* = 1 μm; × 4400

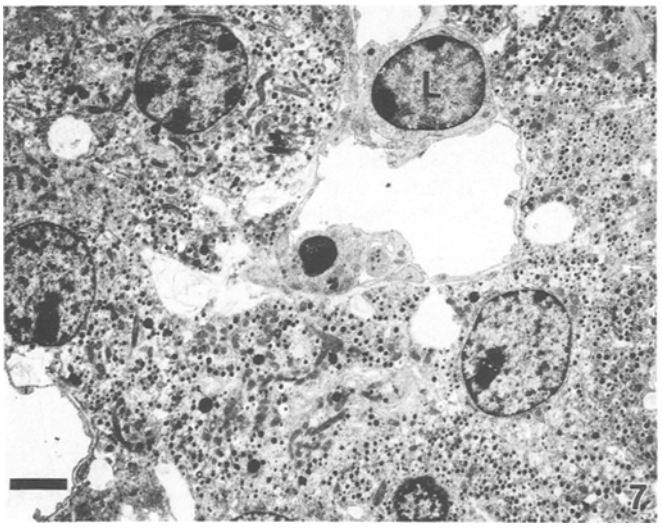

Fig. 7. Photomicrograph showing a lymphocyte (*L*) within the islet parenchyma at day 10. *Bar* = 0.3 μm; × 1500

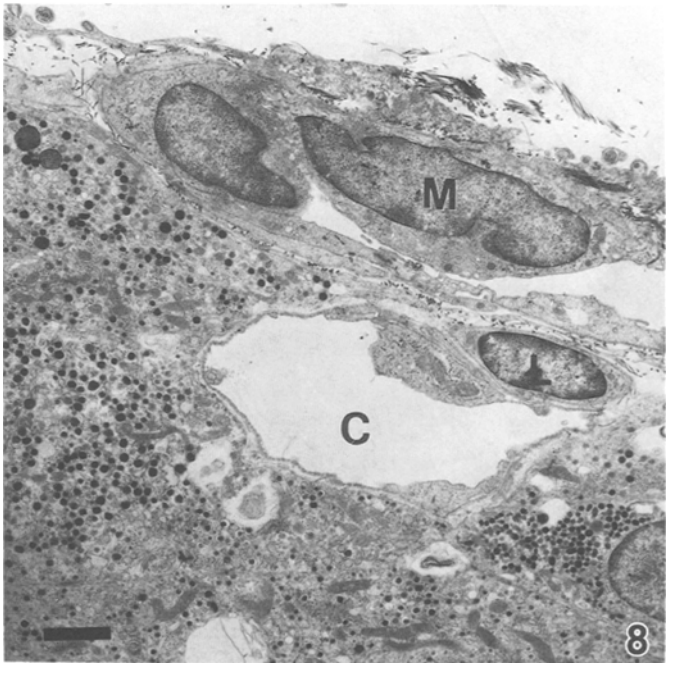

Fig. 8. Photomicrograph showing an intravascular macrophage (*M*) and a lymphocyte (*L*) in a perivascular position at day 15. Capillary lumen (*C*). *Bar* = 0.3 μm; × 1500

spond to hormonal and cellular signals and participate in several physiological and pathological events. They can interact with many extracellular molecules and can internalize and negotiate them for intracellular metabolic changes (Unanue and Allen 1987). Moreover, macrophages are critically situated in the various tissues, usually close to the microvasculature. It is also assumed that during the early islet infiltration monokine production by macrophages causes increased capillary permeability (Nerup et al. 1987, 1989). On this point we have recently demonstrated that during the early LDS treatment reduction in islet capillary area occurs (Papaccio et al. 1990): this observation, together with the finding of phagocyte migration from the blood stream to extravascular sites through capillary walls, is of great importance during the initial stages of the disease.

Kolb-Bachofen et al. (1988) hypothesized that in LDS-treated mice STZ has a dual effect: as a selective islet beta-cell toxin it exerts a direct cytotoxic activity in beta-cells; furthermore it stimulates intra-islet macrophages to develop chemotactic and cytotoxic activities, damaging surrounding still intact islet beta-cells. The effectivness of STZ activity as a direct toxin on islet beta-cells, acting without stimulating autoimmune processes has been already stressed (Papaccio et al. 1991). This effect has also been evident in this study examining ultrastructure where intact beta-cells were seen in the

same islet close to others showing swollen mitochondria, dilated Golgi apparatus and areas of vacuolation other than degranulation; moreover damaged beta-cells were noticed without the close proximity of macrophages or other cytotoxic effector cells. The co-existence of both intact and lysed insulin-containing beta-cells and the lack (in the immediate vicinity) of phagocytes is consistent with the above-reported hypothesis. This important aspect should be taken into consideration when comparing LDS diabetes to other types of autoimmune diabetes.

Our findings are also in accordance with those of Nagy et al. (1988), who affirmed that islet inflammation is dissociated from clinical diabetes onset. This is evident examining blood glucose values that were normal until day 15. Animals only became hyperglycaemic on day 18, when inflammation is maximal and islet beta-cells are mostly damaged or show marked signs of regression.

Acknowledgements. This work was supported in part by the Italian Consiglio Nazionale delle Ricerche (C.N.R.) grant no. 12/06/90/001. The authors thank Professor Pietro M. Motta (Rome) for his reviews, and Mr. Michael Latronico for his expert technical assistance.

References

Charlton B, Bacelj A, Mandel TE (1988) Administration of silica particles or anti-Ly T2 antibody prevents B cell destruction in NOD mice given cyclophosphamide. Diabetes 37:930–935

Groscurth P (1989) Cytotoxic effector cells of the immune system. Anat Embryol 180:109–119

Hanenberg H, Kolb-Bachofen V, Kantwerk-Funke G, Kolb H (1989) Macrophage infiltration precedes and is a prerequisite for lymphocytc insulitis in pancreatic islets of pre-diabetic BB rats. Diabetologia 32:126–134

Kolb H (1987) Mouse models of insulin-dependent diabetes. Low dose streptozocin induced diabetes and NOD mice. Diabetes Metab Rev 3:751–778

Kolb-Bachofen V, Epstein S, Kiesel U, Kolb H (1988) Low-dose-streptozocin induced diabetes in mice. Electron microscopy reveals single-cell insulitis before diabetes onset. Diabetes 37:21–27

Lee KU, Amano K, Yoon JW (1988a) Evidence for initial involvement of macrophages in development of insulitis in NOD mice. Diabetes 37:989–991

Lee KU, Kim MK, Amano K, Pak CY, Jaworski MA, Mehta JG, Yoon JW (1988b) Preferential infiltration of macrophages during early stages of insulitis in diabetes-prone BB rats. Diabetes 37:1053–1058

Like AA, Rossini AA (1976) Streptozocin induced pancreatic insulitis: new model of diabetes mellitus. Science 133:415–417

Like AA, Appel MC, Williams RM, Rossini AA (1978) Streptozocin-induced pancreatic insulitis in mice. Lab Invest 38:470–486

Nagy MV, Chan EK, Teruya M, Forrest LE, Likhite V, Charles MA (1988) Macrophages-mediated islet cell toxicity in BB rats. Diabetes 38:1329–1331

Nerup J, Mandrup-Poulsen T, Molvig J (1987) The HLA-IDDM association: implications for aetiology and pathogenesis of IDDM. Diabetes Metab Rev 3:779–802

Nerup J, Mandrup-Poulsen T, Helqvist S, Wogensen L, Egeberg J (1989) Mechanisms of pancreatic B-cell destruction in type 1 diabetes. Diabetes Care 11 [Suppl 1]:16–22

Papaccio G, Mezzogiorno V (1989) Morphological aspects of glucagon and somatostatin islet cells in diabetic bio breeding and low-dose streptozocin-treated Wistar rats. Pancreas 4:289–294

Papaccio G, Pisanti FA, Frascatore S (1986) Acetyl-homocysteine-thiolactone-induced increase of superoxide-dismutase counteracts the effects of subdiabetogenic doses of streptozocin. Diabetes 35:470–474

Papaccio G, Chieffi Baccari G, Mezzogiorno V, Esposito V (1990) Capillary area in early low-dose-streptozocin treated mice. Histochemistry 95:19–21

Papaccio G, Linn T, Federlin K, Volkman A, Esposito V, Mezzogiorno V (1991) Further morphological and biochemical observations on early low-dose-streptozocin diabetes in mice. Pancreas 6:659–667

Unanue ER, Allen PM (1987) The basis for the immunoregulatory role of macrophages and other accessory cells. Science 236:551–557

Walker R, Bone AJ, Cooke A, Beird JD (1988) Distinct macrophage sub-population in pancreas of prediabetic BB/E rats: possible role for macrophages in pathogenesis of IDDM. Diabetes 37:1301–1304